Molecular Crystals and Liquid Crystals

ISSN: 1542-1406 (Print) 1563-5287 (Online) Journal homepage: http://www.tandfonline.com/loi/gmcl20

Phosphorescence Variation on the Electron Density of Donor Acceptor-type Iridium(III) Complex Ligands

Sang-Yong Park, Sang-Wook Lee & Dong-Myung Shin

To cite this article: Sang-Yong Park, Sang-Wook Lee & Dong-Myung Shin (2015) Phosphorescence Variation on the Electron Density of Donor Acceptor-type Iridium(III) Complex Ligands, Molecular Crystals and Liquid Crystals, 620:1, 132-138, DOI: 10.1080/15421406.2015.1095386

To link to this article: http://dx.doi.org/10.1080/15421406.2015.1095386

Published online: 16 Dec 2015.

Mol. Cryst. Liq. Cryst., Vol. 620: pp. 132–138, 2015

ISSN: 1542-1406 print/1563-5287 online
DOI: 10.1080/15421406.2015.1095386

Phosphorescence Variation on the Electron Density of Donor Acceptor-type Iridium(III) Complex Ligands

SANG-YONG PARK, SANG-WOOK LEE, AND DONG-MYUNG SHIN*

Department of Chemical Engineering, Hong-ik University, Seoul, Korea

Organic light-emitting diodes (OLEDs) using phosphorescent iridium(III) complexes attract enormous attention because they allow highly efficient electrophosphorescence, and the OLED displays and lighting applications market has been growing continually. We synthesized phosphorescent iridium(III) complexes. The donor acceptor-type ligands for the iridium(III) complexes were synthesized by the Suzuki coupling reaction. The ligands, through changes in oxidative addition materials (electron acceptor) and organic borane (electron donor) to obtain the red color, were used to study appropriate iridium(III) complexes. Oxidative addition materials were used, such as 2-bromo-4-(trifluoromethyl)pyridine and 2-bromopyridin-4-amine. Dithieno[3,2-b:2′,3′-d]thiophen-2-ylboronic acid, phenanthren-9-ylboronic acid, and (3-aminophenyl)boronic acid were used as organic borane. Iridium(III) complexes were synthesized through the two steps of the Nonoyama reaction, as well as measured by nuclear magnetic resonance (NMR), UV-visible spectroscopy, and photoluminescence (PL). The phosphorescence emission maxima were dependent on the electron density of the donor and acceptor moieties of the ligands.

Keywords OLED; Iridium(III) complex; Phosphorescent

1. Introduction

Organic light-emitting diodes (OLEDs) using phosphorescent iridium(III) complexes attract enormous attention because they allow highly efficient electro-phosphorescence. Ultra-high-dimension (3840 × 2160) organic light-emitting diodes (UHD OLEDs) have attracted attention regarding the next generation of TVs in the world TV market. Therefore, leading OLED technology is becoming more important [1–2].

OLEDs have many advantages. They can be fabricated as lightweight, thin, and flexible. In addition, they have good battery power efficiency, a faster response time, a greater artificial contrast ratio, and a wider viewing angle compared to liquid crystal displays (LCDs), because OLED pixels emit light directly [3–8].

OLEDs are composed of a glass substrate, transparent conductor (ITO), electron injection layer (EIL), electron transfer layer (ETL), emission material layer (EML), hole

*Address correspondence to D. M. Shin, Department of Chemical Engineering, Hong-ik University, 94, Wausan-ro, Mapo-gu, Seoul, Korea. E-mail: shindm@hongik.ac.kr

Color versions of one or more of the figures in the article can be found online at www.tandfonline.com/gmcl.

transfer layer (HTL), hole injection layer (HJL), and metal cathode [9]. We have been studying phosphorescent iridium(III) complex dopants for the EML layer. The excitons formed in EML are composed of 25% singlet and 75% triplets, which both enable a nearly 100% internal device quantum efficiency [10–14]. Such promising features prompted the development of a number of novel phosphorescent iridium(III) complexes.

We focused on the synthesis methods of red phosphorescent dopant materials. In this paper, we report the synthesis and emission properties of novel red-emitting iridium(III) complexes through changed electron donor and electron acceptor ligand and measurement characteristics, respectively.

2. Experimental Details

2.1. General Information

All reactions and manipulations were carried out under N_2 with the use of a standard inert atmosphere. Solvents were dried by standard procedures. All column chromatography was performed under a standard atmosphere with the use of silica gel (230–400 mesh, Sigma-Aldrich) or aluminum oxide (Sigma-Aldrich) as the stationary phase in a column 30 cm long and with a 2.0-cm diameter. The ^{1}H NMR spectra were measured using a Bruker DRX 400 spectrometer in a deuterated chloroform solution. In addition, 500 MHz of UV–visible absorption spectra were recorded on an Agilent 8453 UV–Vis spectrophotometer. All measurements were carried out at room temperature. To determine the expected phosphorescent emission energy and electronic state of the newly designed iridium complex, we used the Gaussian 09 program, which performs structure optimization and time-dependent density functional theory (TD-DFT) calculations HF and DFT.

2.2. Synthesis of the Main Ligands

The ligands were synthesized by essentially following the same procedure, and an illustrative example is provided at Scheme 1.

2-(dithieno[3,2-b:2′,3′-d]thiophen-2-yl)-4-(trifluoromethyl)pyridine (DTT-TFP). A mixture of 2-bromo-4-(trifluoromethyl)pyridine (1.04 g, 4.58 mmol), dithieno[3,2-b:2′,3′-d] thiophene-2-boronic acid (1.00 g, 4.16 mmol), $Pd(PPh_3)_4$ (0.19 g, 0.167 mmol, 4 mol%), anhydrous sodium carbonate (1.73 g, 12.5 mmol), aliquat 336 (0.67 g, 1.67 mmol), tetrahydrofuran (80 mL), and water (50 mL) was headed under a nitrogen atmosphere at 80°C for 24 h. This reaction is the Suzuki coupling reaction. After, the organic mixture solids were collected by a glass filter (G4), the reaction mixture was washed with hexane, water, and methanol several times and dried in a vacuum. Yield: 53.6% (0.766 g); ^{1}H NMR ($CDCl_3$, 500 MHz): δ_H(ppm) 8.47(s, 1H), 8.12(s, 1H), 7.51(s, 1H), 7.25(s, 1H), 7.25(s, 1H), 6.96(s, 1H).

2-(dithieno[3,2-b:2′,3′-d]thiophen-2-yl)pyridine-4-amine (DTT-PA). A DTT-PA ligand was obtained from the reaction of 2-bromopyridine-4-amine (0.79 g, 4.58 mmol) and dithieno[3,2-b:2′,3′-d] thiophene-2-boronic acid (1.00 g, 4.16 mmol) by Suzuki coupling. The abstraction and purification processes are the same as described above. Yield: 51.3%

(0.62 g); ^{1}H NMR ($CDCl_3$, 500 MHz): δ_H(ppm) 8.32(s, 1H), 7.25(s, 1H), 7.20(s, 1H), 6.96(s, 1H), 6.86(s, 1H), 6.65(s, 1H), 6.27(d, 2H).

2-(phenanthren-9-yl)-4-(trifluoromethyl)pyridine (PT-TFP). A PT-TFP ligand was obtained from the reaction of 2-bromo-4-(trifluoromethyl)pyridine (1.12 g, 4.95 mmol) and 9-phenanthrylboronic acid (1.00 g, 4.5 mmol) by Suzuki coupling. The abstraction and purification processes are the same as described above. Yield: 89.3% (1.30 g); ^{1}H NMR ($CDCl_3$, 500 MHz): δ_H(ppm) 8.93(s, 2H), 8.44(s, 1H), 8.38(s, 1H), 8.12(s, 2H), 8.06(s, 1H), 7.88(s, 2H), 7.82(s, 2H), 7.25(s, 1H).

3-(4-(trifluoromethyl)pyridine-2-yl)aniline (TFP-AN). A PT-TFP ligand was obtained from the reaction of 2-bromo-4-(trifluoromethyl)pyridine (1.82 g, 8.03 mmol) and (3-aminophenyl)boronic acid (1.00 g, 7.30 mmol) by Suzuki coupling. The abstraction and purification processes are the same as described above. Yield: 87.4% (1.52 g); ^{1}H NMR ($CDCl_3$, 500 MHz): δ_H(ppm) 8.38(s, 1H), 8.06(s, 1H), 7.66(s, 1H), 7.47(s, 1H), 7.15(s, 1H), 6.65(s, 1H), 6.27(d, 2H).

2.3. Synthesis of the Cyclometalated Iridium(III) μ-Chloride-Bridged Dimer

All Dimers were synthesized by essentially following the same procedure, and an illustrative example is provided at Scheme 1.

Dimer [(DTT-TFP)$_2$IrCl]$_2$ diiridium(III). The cyclometalated iridium(III) μ-chloride-bridged dimer, [(DTT-TFP)$_2$Ir(μ-Cl)]$_2$ (II), was prepared using a slightly modified Nonoyama reaction step 1. Iridium(III) chloride hydrate (0.333 g, 1.12 mmol) and DTT-TFP (0.766 g, 2.23 mmol) were dissolved in a mixed solution of 2-ethoxyethanol and water (3:1 vol%, 40 mL). The reaction was required under a nitrogen atmosphere. The mixture was refluxed overnight at 135°C. The solution was cooled to room temperature and the flask was left in an ice bath for 2 h. Afterwards, the mixture was diluted with an additional 2,000 mL of water and the organic layer separated was collected by a G4 glass filter. The precipitation was collected and washed with water and hexane several times. Yield: 95.7%.

Dimer [(DTT-PA)$_2$IrCl]$_2$ diiridium(III). The cyclometalated iridium(III) μ-chloride-bridged dimer, [(DTT-PA)$_2$Ir(μ-Cl)]$_2$ (II), was obtained from the reaction of iridium(III) chloride hydrate (0.32 g, 1.07 mmol) and DTT-TFP (0.62 g, 2.14 mmol) by the Nonoyama reaction step 1. The abstraction and purification processes are the same as described above. Yield: 91.1%.

Dimer [(PT-TFP)$_2$IrCl]$_2$ diiridium(III). The cyclometalated iridium(III) μ-chloride-bridged dimer, [(PT-TFP)$_2$Ir(μ-Cl)]$_2$ (II), was obtained from the reaction of iridium(III) chloride hydrate (0.6 g, 2.01 mmol) and DTT-TFP (1.30 g, 4.02 mmol) by the Nonoyama reaction step 1. The abstraction and purification processes are the same as described above. Yield: 71.1%.

Dimer [(TFP-AN)$_2$IrCl]$_2$ diiridium(III). The cyclometalated iridium(III) μ-chloride-bridged dimer, [(TFP-AN)$_2$Ir(μ-Cl)]$_2$ (II), was obtained from the reaction of iridium(III) chloride hydrate (0.95 g, 3.19 mmol) and DTT-TFP (1.52 g, 6.38 mmol) by the Nonoyama reaction step 1. The abstraction and purification processes are the same as described above. Yield: 87.4%.

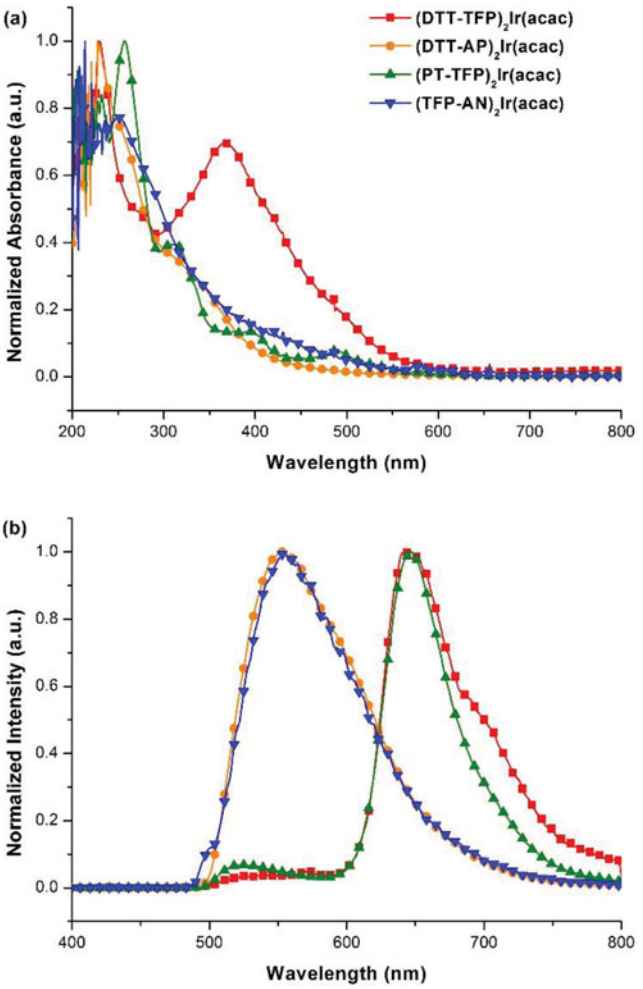

Figure 1. (a) UV–Vis absorption and (b) photoluminescence spectrum of iridium(III) complexes in a $CHCl_3$ solution.

2.4. Preparation of the Iridium(III) Complexes

All the cyclometalated iridium(III) complexes were prepared by essentially following the same procedure, and an illustrative example is provided at Scheme 1.

$(DTT\text{-}TFP)_2Ir(acac)$ complex: The $[(DTT\text{-}TFP)_2Ir(\mu\text{-}Cl)]_2$ (II) (0.970 g, 0.534 mmol), acetylacetone (0.107 g, 1.07 mmol), and sodium carbonate (0.184 g, 1.36 mmol) were dissolved in 2-ethoxyethanol (77.6 ml) and refluxed under a nitrogen atmosphere overnight at 135°C. After cooling to room temperature, the flask was left in an ice bath for 2 h. The crude reaction product was poured into water, extracted with dichloromethane, and the extract was concentrated under a vacuum. The product was purified by column chromatography (silica gel, methanol: CH_2Cl_2 = 1:20). Yield: 61.2%;

Table 1. UV–Vis absorption and photoluminescence spectrum peaks of iridium(III) complexes

Complexes	UV Absorption λ (nm)			PL Emission λ (nm)
	First peak	Second peak	Third peak	Maximum peak
$(DTT\text{-}TFP)_2Ir(acac)$	230	367	486	647
$(DTT\text{-}PA)_2Ir(acac)$	230	422	483	553
$(PT\text{-}TFP)_2Ir(acac)$	257	310	393	647
$(TFP\text{-}AN)_2Ir(acac)$	250	386	490	552

^{1}H NMR ($CDCl_3$, 500 MHz): δ_H(ppm) 8.42(s, 2H), 8.12(s, 2H), 7.51(s, 2H), 7.20(s, 2H), 6.96(s, 2H), 5.25(s, 1H), 2.24(t, 6H).

The $(DTT\text{-}PA)_2Ir(acac)$ complex was obtained from the reaction of $[(DTT\text{-}PA)_2Ir(\mu\text{-}Cl)]_2$ (II) (0.78 g, 0.49 mmol) and acetylacetone (0.01 g, 0.97 mmol) by the Nonoyama reaction step 2. The abstraction and purification processes are the same as described above. Yield: 70.4%; ^{1}H NMR ($CDCl_3$, 500 MHz): δ_H(ppm) 8.50(s, 2H), 7.20(s, 2H), 6.96(s, 2H), 6.86(s, 2H), 6.65(s, 2H), 6.27(d, 4H), 5.75(s, 1H), 2.24(t, 6H).

The $(PT\text{-}TFP)_2Ir(acac)$ complex was obtained from the reaction of $[(PT\text{-}TFP)_2Ir(\mu\text{-}Cl)]_2$ (II) (1.23 g, 0.71 mmol) and acetylacetone (0.14 g, 1.41 mmol) by the Nonoyama reaction step 2. The abstraction and purification processes are the same as described above. Yield: 66.3%; ^{1}H NMR ($CDCl_3$, 500 MHz): δ_H(ppm) 8.9∼7.8(m, 16H), 8.33(s, 2H), 8.06(s, 2H), 7.15(s, 2H), 5.75(s, 2H), 2.24(t, 6H).

The $(TFP\text{-}AN)_2Ir(acac)$ complex was obtained from the reaction of $[(TFP\text{-}AN)_2Ir(\mu\text{-}Cl)]_2$ (II) (1.94 g, 1.38 mmol) and acetylacetone (0.277 g, 2.76 mmol) by the Nonoyama reaction step 2. The abstraction and purification processes are the same as described above. Yield: 71.7%; ^{1}H NMR ($CDCl_3$, 500 MHz): δ_H(ppm) 8.33(s, 2H), 8.06(d,2H), 7.40(s, 2H), 7.28(s, 2H), 7.15(s, 1H), 6.65(s, 2H), 6.27(d,4H), 5.75(s, 1H), 2.24(t, 6H).

3. Results and Discussion

3.1. Iridium Complex Properties

Figure 1 shows the UV–Vis absorption and photoluminescence (PL) emission spectrum of the iridium complexes in a chloroform solution at room temperature. Table 1 shows spectrum peaks of Figure 1(a) and Figure 1(b). The triplet transition state is responsible for the observed phosphorescence, and it is generally accepted to describe the phosphorescence emission according to Kasha's rule [15]. Therefore, the lowest triplet state is the spin-forbidden metal-to-ligand charge transfer (^{3}MLCT) transition and the triplet ligand centered (^{3}LC) transition states. ^{3}MLCT and ^{3}LC transition states are close to the third peak [16]; therefore, the maximum peaks of the PL emission spectrum are observed clearly, when the complexes absorbed light at the third UV–Vis spectrum peak [17].

$(DTT\text{-}TFP)_2Ir(acac)$ and $(DTT\text{-}PA)_2Ir(acac)$ emitted phosphorescence at 647 nm and 553 nm, respectively. $(DTT\text{-}TFP)_2Ir(acac)$ and $(DTT\text{-}PA)_2Ir(acac)$ have the same electron

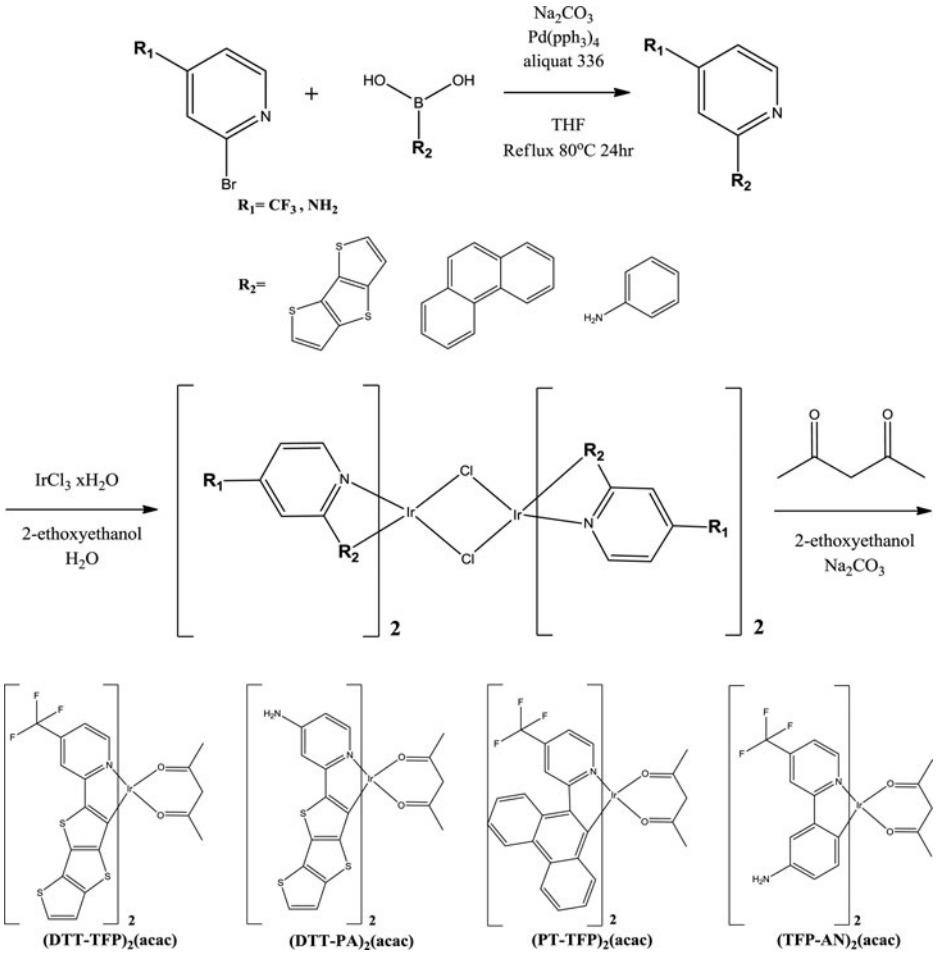

Scheme 1. Synthetic route of main ligands and their iridium(III) complexes.

donor (dithieno[3,2-b:2′,3′-d]thiophen, DTT) as the main ligand. DTT formed high conjugation, and a high electron density according to high conjugation should increase the highest occupied molecular orbital (HOMO) energy level. These complexes have different electron acceptors (pyridine group). Furthermore, the $–CF_3$ and $–NH_2$ functional group showed different characteristics, while $–CF_3$ is an efficient electron-withdrawing group. Therefore, the electron density in the pyridine ring is decreased and the lowest unoccupied molecular orbital (LUMO) energy level is decreased. Therefore, the HOMO-LUMO energy gap of (DTT-TFP)$_2$Ir(acac) is decreased and the emission wavelength is increased. Alternatively, unshared electron pairs of the -NH_2 functional group increase the electron density of the pyridine ring. Therefore, the LUMO energy level is increased and the HOMO-LUMO energy gap of (DTT-PA)$_2$Ir(acac) is increased.

(PT-TFP)$_2$Ir(acac) and (TFP-AN)$_2$Ir(acac) have different electron donors. The phenanthren has a high electron density because it becomes high conjugation in the phenanthren rings. Therefore, it increased the HOMO energy level. Relatively, aniline does not have a high electron density and it has a low HOMO energy level. Therefore, the maximum PL

peak of $(PT\text{-}TFP)_2Ir(acac)$ was observed at 647 nm and the relatively blue-shifted maximum PL peak of $(TFP\text{-}AN)_2Ir(acac)$ was observed at 552 nm.

4. Conclusion

As a result of a simulation using the Gaussian 09 program, $(DTT\text{-}TFP)_2Ir(acac)$, $(DTT\text{-}PA)_2Ir(acac)$, $(PT\text{-}TFP)_2Ir(acac)$, and $(TFP\text{-}AN)_2Ir(acac)$ were predicted to emit luminance at 638.39 nm, 597.22 nm, 645 nm, and 643.58 nm, respectively. When iridium(III) complexes were synthesized and the maximum PL of $(DTT\text{-}TFP)_2Ir(acac)$ was observed at 647 nm at room temperature, the maximum PL values of $(DTT\text{-}PA)_2Ir(acac)$, $(PT\text{-}PFP)_2Ir(acac)$, and $(TFP\text{-}AN)_2Ir(acac)$ were observed at 553 nm, 647 nm, and 552 nm, respectively. As a result, it was confirmed that $(DTT\text{-}TFP)_2Ir(acac)$ and $(PT\text{-}PFP)_2Ir(acac)$ are suitable for a deep red-emitting iridium(III) complex.

Acknowledgments

This work was supported by the Technology Innovation Program (201210940003, Materials Development for 50-inches UD OLED TV Using Super Hybrid Process) and funded by the Ministry of Knowledge Economy (MKE, Korea).

References

[1] You, Y. M., & Park, S. Y. (2009). *Dalton Trans.*, *8*, 1267.
[2] Brown, J. *et al.* (2012). Article first published online, *10*, 1889.
[3] D'Andrade, B. W. & Forrest, S. R. (2004). *Adv. Mater.*, *16*, 1585.
[4] Lim, S. H. *et al.* (2008). *Mol. Cryst. Liq. Cryst.*, *491*, 40.
[5] Ryu, G. Y. *et al.* (2009). *Mol. Cryst. Liq. Cryst.*, *499*, 75.
[6] Park, N. R. *et al.* (2011). *Mol. Cryst. Liq. Cryst.*, *538*, 75.
[7] Lee, S. N. *et al.* (2013). *Mol. Cryst. Liq. Cryst.*, *587*, 59.
[8] Lee, S. N. *et al.* (2014). *J. Nanosci. Nanotechnol.*, *14*, 6185.
[9] Geffroy, B. *et al.* (2006). Article first published online, *10*, 1002.
[10] Liang, B. *et al.* (2006). *J. Mater. Chem.*, *16*, 1281.
[11] Marin, V. *et al.* (2007). *Chem. Soc. Rev.*, *36*, 618.
[12] Chou, P. T., & Chi, Y. (2007). *Chem.–Eur. J.*, *13*, 380.
[13] Rehmann, N. *et al.* (2007). *Appl. Phys. Lett.*, *91*, 103507.
[14] Schwartz, G. *et al.* (2009). *Adv. Funct. Mater.*, *19*, 1319.
[15] Tsuboi, T. *et al.* (2008). *Jpn. J. Appl. Phys.*, *47*, 1266.
[16] Li, J. *et al.* (2005). *Inorg. Chem.*, *44*, 1713.
[17] Shin, D. M. (2014). *Sci. Adv. Mater.*, *6*, 1.